Static Structural Analyses Considering True Yield Stress of Alloy Wheel Materials by Finite Element Method

Bhaskar Ohol[1], Ayush Kumar[2], Chaitali Nangare[3], Manasi Lavate[4], Varsha Patil[5]
[1,2,3,4,5]*Padmabhooshan Vasantdada Patil Institute of Technology, Pune 411021, India*

Abstract—**This study focuses on verification of strength of design for alloy wheels with two different materials viz. magnesium alloy AZ80 and aluminium alloy 7075 T6 considering static loading conditions. An alloy wheel of 15-inch diameter is considered based on the standard alloy wheel used in hatchback cars by the different auto manufacturers. The static structural analysis considering the true yield stress values of the alloy wheel materials are performed using the Finite Element Method (FEM). The ability of FEM to model subtle changes in geometry allows to optimize size, shape, or form to obtain minimum weight or maximum performance. Yielding of material is considered as failure of the alloy wheel material. As per the yield criterion concluded that that the magnitude of maximum von Mises stress should not exceed 570 MPa and 275 MPa for aluminium and magnesium alloys respectively under the maximum static radial load of 9000N including the weight of vehicle, passengers and inflated air pressure. The analysis pin points the edge portion of the alloy wheels needs to be strengthened as it invariably shows more resultant displacement. The advantage of this study is that it verifies the strength of design of alloy wheels and suggests future study considering the coupled effect of static vehicle weight, cornering, braking, acceleration, and the tire inflation pressure on the alloy wheel for an improved geometric configuration for alloy wheels.**

Index Terms—**alloy wheel; static loading; finite element method; von Mises stress; strength of design**

I. INTRODUCTION

Alloy wheels used for passenger cars are essential to automobiles for carrying passengers safely and comfortably. Alloy wheels have a symmetrical geometry and are grouped into four types, namely disc type, spoke type, fin type, and mesh type, respectively, including principal components such as rim and wheel disc, as shown in Figure 1. Each wheel bears the load of the vehicle in balance with static and dynamic loads depending on the parameters viz. carrying weight, velocity, and road surface. By the virtue of these loads, there is apprehension about the reliability and safety of the alloy wheel structure, and its geometric parameter is important to be verified for the safety requirements and standards. By and large, a passenger car wheel must satisfy the standard tests prior to mass production - the dynamic radial fatigue test, the dynamic cornering fatigue test, and the impact test. However, mechanical engineering design and wheel analysis require predicting deformation and fatigue failure before pilot model testing [1]. The mechanical design of alloy wheels with Finite Element Analysis (FEA) simulation is imperatively utilized for fatigue life prediction, because it is more flexible for modelling part geometries, applying material properties, and types of load. Strength analysis of alloy wheel materials, such as magnesium and aluminium for passenger cars using the FEA model, is performed to determine the optimal geometry and mass under a dynamic load. The results reveal that the aluminium alloy is superior in terms of ultimate strength. From the fatigue strength test, aluminum alloy is the best material for lightweight wheels. The magnesium alloy wheel shows failure in the shortest fatigue cycle; however, the aluminum wheel can withstand the complex dynamic load, exhibiting load fatigue life. Stress analysis from the FEA results revealed that maximum stress concentration is represented around the connecting area between the rim and the drop centre, where the rim plays a role as the first support of radial load from tires [2,3].

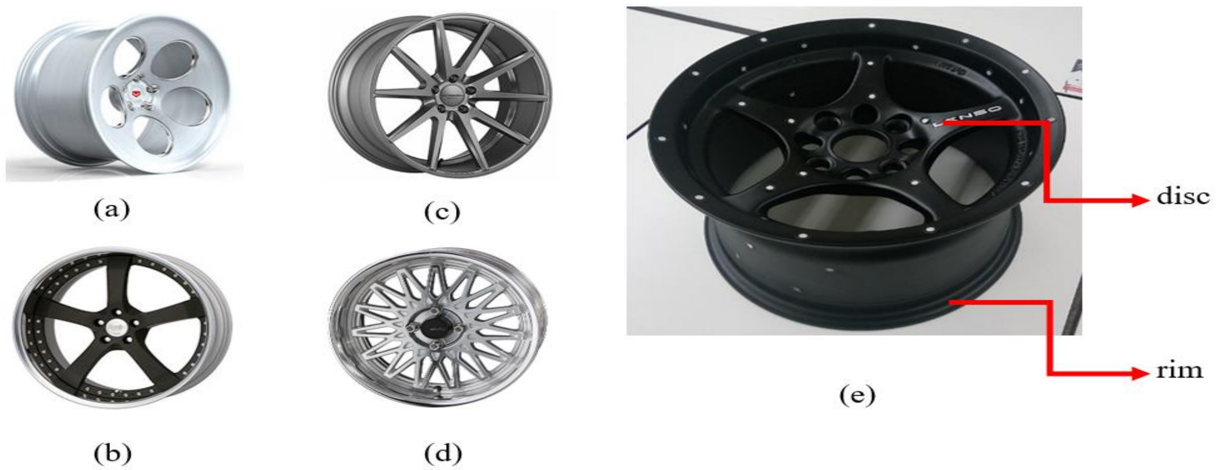

Figure 1. Type of alloy wheel in general industry and components. (a) Disc type, (b) spoke type, (c) fin type, (d) mesh type, and (e) rim and disc type.

Geometrical optimization of alloy wheels through validation of FEA simulation models with actual experiments under static load was carried out by many researchers in past. P. Rammurty et al. [4] performed an experiment fatigue test of aluminium alloy 356.2 T2 of alloy wheel to find a correlation between stress and fatigue for taking properties of it to apply to FEA, and compared the result from simulations against Japan Light Alloy Wheel Standard ISO 3006:2015. The result showed that test was satisfactory; in addition, this FEA modeling could be utilized to estimate life cycle of 356.2 T2 alloy wheel. Liangmo Wang et al. [5] improved the dimension of alloy wheels to avoid maximum stress around screw holes by using FEA to predict the fatigue life cycle for decreasing cost before manufacturing. Xiaofeng Wang et al. [6] studied the dynamic cornering fatigue test prediction by the fundamental failure theory of alloy wheels and calculation of fatigue life considering bilinear isotropic hardening, multi-axis fatigue, and rain-flow counting the Palmgren-Miner rule; the crack area of the alloy wheel from FEA was consistent with the experiment. Dong [7] designed the shape of an alloy wheel under dynamic cornering fatigue test with FEA by considering stress distribution and deformation on the alloy wheel, simulated fatigue life according to transient structural with cyclic loading, and analyzed design variables of alloy wheel by response surface method with nine initial sampling from design of experiment. Sourav Das [3] diagnosed the weight loss of the alloy wheel by applying FEA with radial loading distribution and determined AlSi as a material of the alloy wheel. The radial fatigue test, cornering fatigue test, and impact test were considered using the FE simulation, and the result depicted that the optimal shape of the alloy cut its weight but still passed the standard fatigue test. D.H. Burande and T.N. Kazi [8] performed an alloy wheel with dynamic cornering fatigue test and radial fatigue test following ISO 3006:2015, using FE simulation, which compared two material types, namely aluminium A356 and aluminum 7075-T6 on both methods; the result showed that aluminum A356 provided FEA result was close to experiment rather than another. Rakesh B. Thakare [9] executed a type alloy wheel on FEA with a dynamic cornering fatigue test for comparing strain against an experiment under the Society of Automotive Engineering (SAE) standard, aimed around holes fixing between wheel and disc, and both results were agreeable.Of late, many researchers attempted to perform FEA and experiment alloy wheels as per the international standards. From these studies, it is understood that the static stress analysis is necessary to be performed by applying material true stress-strain values so as to obtain the realistic response of the alloy wheel materials. Dealing with a complex stress state and varying geometric configuration, the von Mises failure criterion is applied to decide the structural integrity of the material. Since the stress levels in the wheel are within the elastic region of the material for the considered loading condition, a stress-based approach has been followed.

II. METHODOLOGY

2.1 True Stress- Strain and Engineering True Stress-Strain To understand the plastic flow of the materials of alloy wheels, true stress-true strain curves at 0.000625 $^{-1}$ (quasi-static strain rate) were plotted applying the following equations:

$$\varepsilon = \ln(e+1) \tag{1}$$

where, ε is true strain and e is conventional or engineering strain.

$$\sigma = s(1+e) \tag{2}$$

where, σ is true stress and s is conventional or engineering stress. The true stress-true strain curves of the materials are shown in Fig.3, Fig.4 and Fig.5.

2.2 Equivalent Stress and Equivalent Strain

Considering a complex stress condition during radial loading and the material of the alloy wheel being ductile, the von Mises or Distortion Energy criterion was applied to understand the effective deformation of the projectile. The conversion of a uniaxial stress state into a multiaxial stress condition is accomplished by the use of the equivalent stress and strain [8].

The von Mises expressions for equivalent stress($\bar{\sigma}$) and equivalent strain($\bar{\varepsilon}$) are represented as under: -

Equivalent stress $(\bar{\sigma}) =$

$$\sqrt{\frac{1}{2}[(\sigma_1-\sigma_2)^2 - (\sigma_2-\sigma_3)^2 - (\sigma_3-\sigma_1)^2]} \tag{3}$$

where, σ_1, σ_2 and σ_3 are the principal stresses.

Equivalent strain $(\bar{\varepsilon}) =$

$$\frac{1}{3}\sqrt{2\,[(\varepsilon_1-\varepsilon_2)^2 - (\varepsilon_2-\varepsilon_3)^2 - (\varepsilon_3-\varepsilon_1)^2]} \tag{4}$$

Where, ε_1, ε_2 and ε_3 are the principal strains.

2.3 Yield criterion

Here, von Mises equivalent stress ($\bar{\sigma}$) is taken as effective stress. When von Mises equivalent stress ($\bar{\sigma}$) is equal to or exceeds the yield tensile strength value σ_{yt} , the material is regarded as yielded.

$$\bar{\sigma} \geq \sigma_{yt} \tag{5}$$

III. NUMERICAL METHOD

3.1 Finite Element Analysis

Finite Element Analysis (FEA) is a numerical method applied for structural analysis of engineering bodies with user-defined geometry. Interpolation functions are used to reduce the behavior at an infinite field of points to a finite number of points. The interconnectivity of these points is defined by finite elements that fill the appropriate geometry. The genius of the finite element method is that it enables the systematic solution of these field problems with as much fidelity to geometry as needed. The ability to model subtle changes in geometry permits the optimization of size, shape, or form to obtain minimum weight or maximum performance.

Finite element pre-processing comprises geometry definition and manipulation, specification of material properties, generation of the finite element mesh, and definition of generalized loads and displacements both at the boundary and distributed through the body (inertia and gravitational loads). Note that material properties may be specified as constant or variable. When variable, they are often input as tables of properties or as mathematical functions, such as exponentials. Finite element pre-processing may consume as much as 80% of the calendar time in the finite element process.

3.2 Finite Element Analysis Flow Chart

Typical Finite Element Analysis Procedure mentioned in Figure 2 to be followed in Computer Aided Engineering (CAE) software involves the following steps [10]

(i) Pre-processes: - It comprises geometry definition and manipulation, specification of material properties, generation of finite element mesh, and definition of generalized loads and displacements both at the boundary and distributed through the body.

(ii) Process: - It involves the computation. The CAE software conducts the numerical analysis;

(iii) Post process: - The user sees and interprets the results of the analysis.

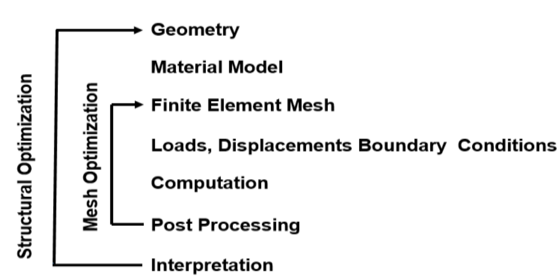

Figure 2. Finite Element Analysis Flow Chart

3.3 Material Model and Finite Element Mesh

A finite element analysis of an axisymmetrical 15-inch diameter magnesium alloy AZ80 and aluminium alloy 7075 T6 was performed in this study. The model of alloy wheel along with the three dimensions under study are shown in Figure 3. It was assumed that the materials were possessing linear elastic homogenous isotropic properties. Magnesium alloy AZ80 is a high-strength, heat-treatable wrought alloy used mainly for structural components of automobiles and aerospace extrusions and forgings. Magnesium alloy AZ80 offers superior mechanical properties, including high strength, good ductility, and fatigue resistance. Al 7075-T6 is a high-strength aluminum alloy, commonly used in high-stress applications, offering properties comparable to many mild steels while maintaining a low density of 2.81 g/cm³ (approx). Due to high strength to weight ratio and excellent fatigue strength, this alloy is preferred in manufacturing of alloy wheels besides aerospace and defence applications. The properties of the magnesium alloy AZ80 [10] and Aluminum 7075-T6 [11] are given in Table 1. Complete assembly is discretized into elements by using following mesh conditions and the mesh control is applied at necessary locations. A mapped meshed model is shown in Figure 4. Mesh convergence is obtained by increasing the size of mesh. The graph

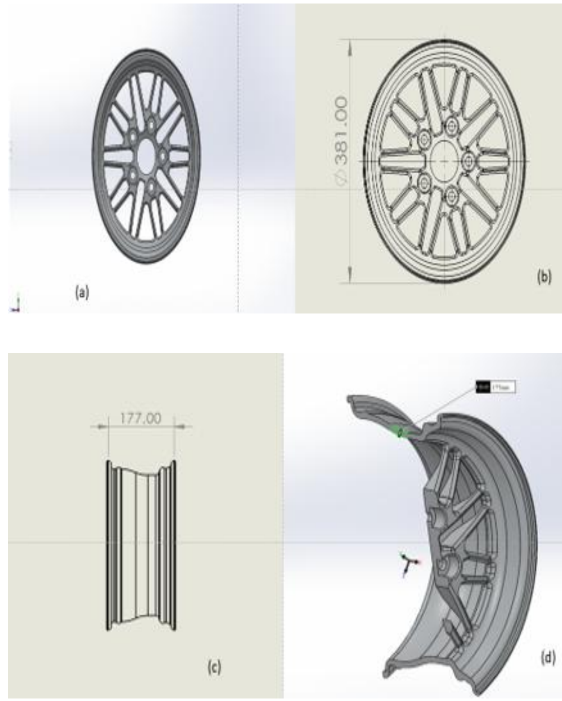

Figure 3. (a) Model of Alloy Wheel, (b) Diameter of the Alloy Wheel, (c) Width of Alloy Wheel and (d) Thickness (min) of Alloy Wheel

Table 1. Mechanical properties of Magnesium alloy AZ380 and Aluminum alloy 7075 T6 [10,11]

Material	Modulus of Elasticity	Poisson's Ratio	Density g/cm^3	True Yield Strength (MPa)	Tensile Strength (MPa)	% Elongation
Magnesium alloy AZ380	44.8GPa	0.35	1.80g/cm^3	275MPa	380MPa	7%
Aluminum alloy 7075 T6	71.7GPa	0.33	2.81g/cm^3	503MPa	572MPa	11%

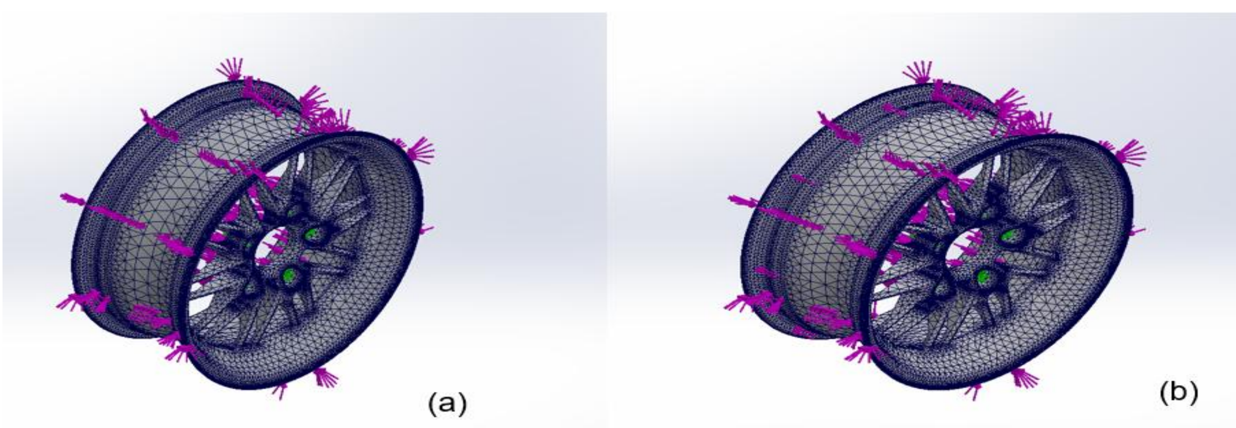

Figure 4. Meshed Models - (a) Al Alloy wheel & (b) Mg Alloy Wheel

Table 2. Mesh Details

Alloy Wheel	Mesh Type	Mesher Used	Jacobian Points	Max Element Size	Min Element Size	Total Nodes	Total Elements
Al Alloy Wheel	Solid Mesh	Curvature based Mesh	At nodes	8.38mm	0.41mm	328896	196506

3.4 Boundary Conditions

It is considered that each wheel of four-wheeler carries equal load; the radial load of 9000N is uniformly applied on the outer portion of the alloy wheel. This loading condition is selected to examine the material strength under the uniformly distributed load as This The alloy wheel is constrained at the five bolt holes, thus fixing all DOFs of the alloy wheel as shown in Figure 5. Mesh convergence is obtained by increasing the size of mesh. The graphs of von-Mises stress versus mesh size are shown in Figure 6.

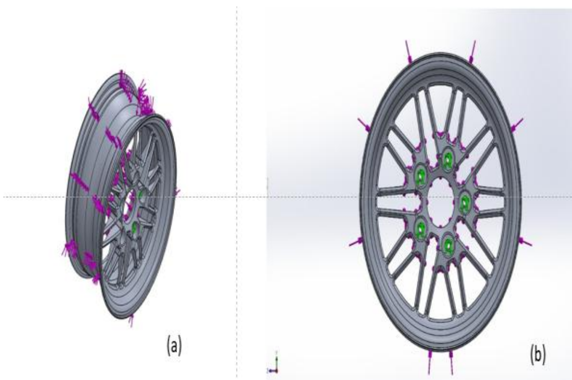

Figure 5. (a) Radial Load on the inner portion of alloy wheel & (b) Fixtures at the holes of Alloy Wheel

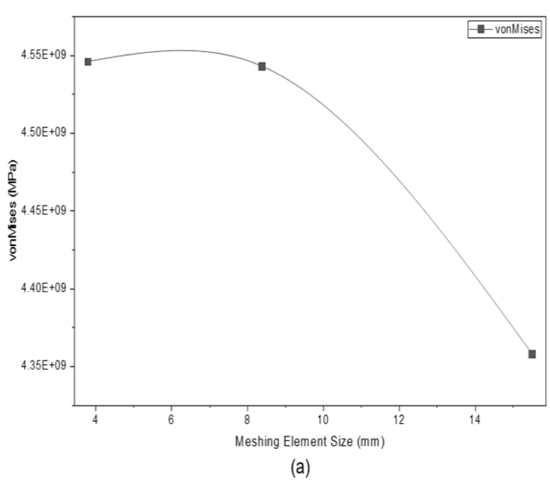

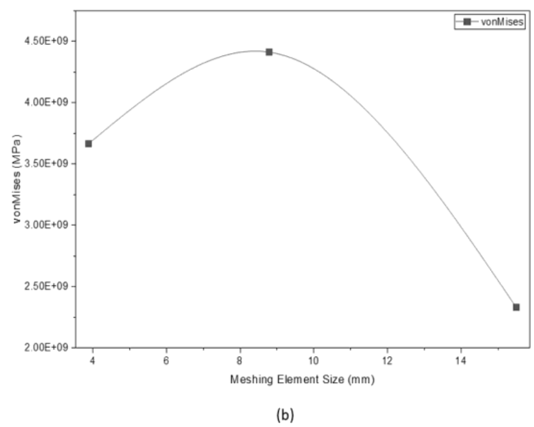

Figure 6. Mesh convergence (a) Al alloy wheel & (b) Mg alloy wheel

IV. RESULTS AND DISCUSSION

Static analysis is performed using radial loading condition to determine the strength of the alloy wheel. The stress and resultant displacement on the wheel at loading condition are found out. Table 3 shows the stress and resultant displacement of the alloy wheels obtained from the FEA.

Material	von Mises Stress MPa	Displace ment mm.	Material True Yield Stress MPa
Magnesium alloy AZ380	Within limit	3.138	275
Aluminum alloy 7075 T6	Within limit	2.322	503

Table 3. Results of Static Structural Analysis

The static stress analysis shows the alloy wheel materials response to the radial load applied uniformly on the outer portion of the alloy wheels. The von Mises stress, equivalent strain and resultant displacement plots obtained are shown in Figure 7 and 8. The maximum equivalent strains values are negligible which shows that the material has not permanently yielded. However, the von-Mises stresses are observed to be more at the curvature portion of the rib at the hub of both the alloy wheels. The resultant displacement is observed invariably abnormal at the edge portion of the alloy wheel.

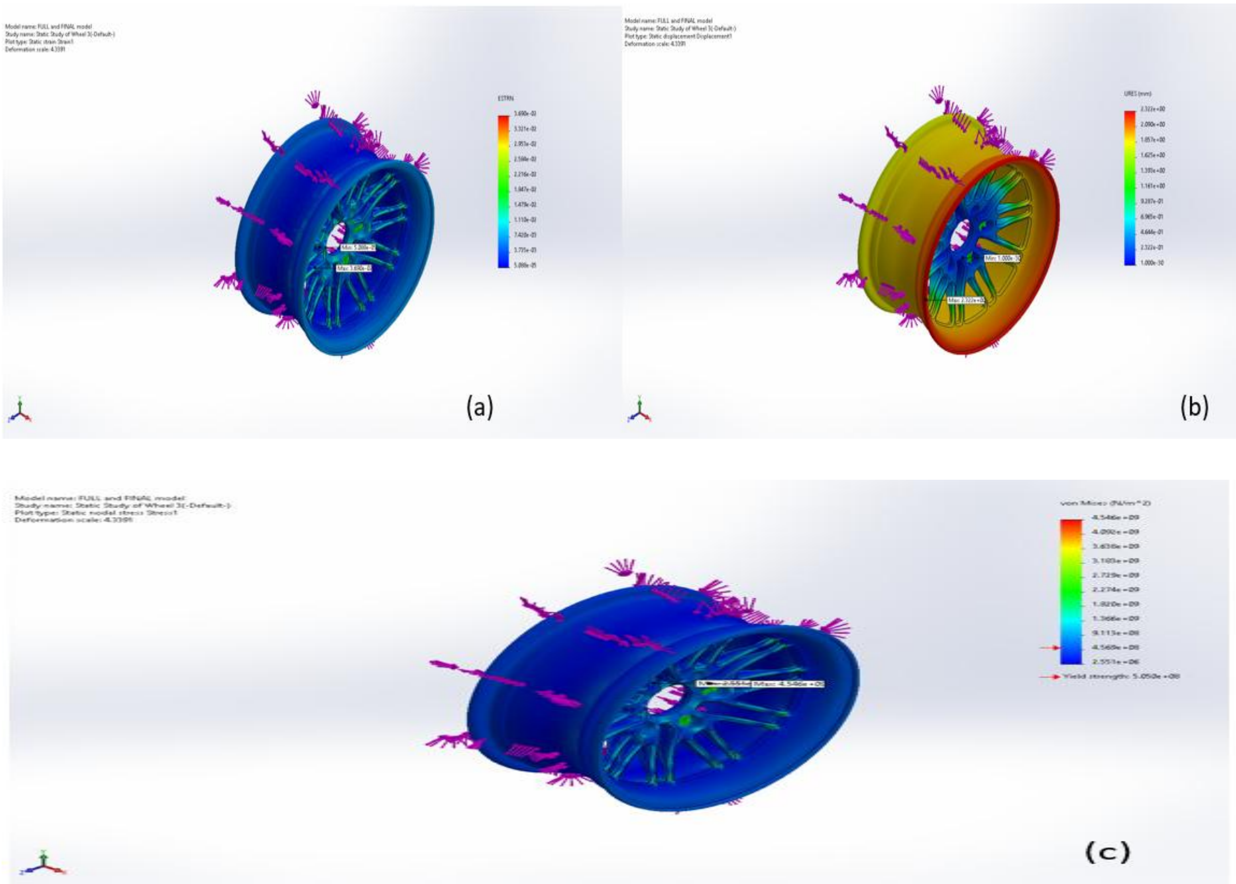

Figure 7. Stress-strain plots- Al alloy wheel (a) Equivalent strain plot, (b) Displacement plot & (c) von-Mises stress plot

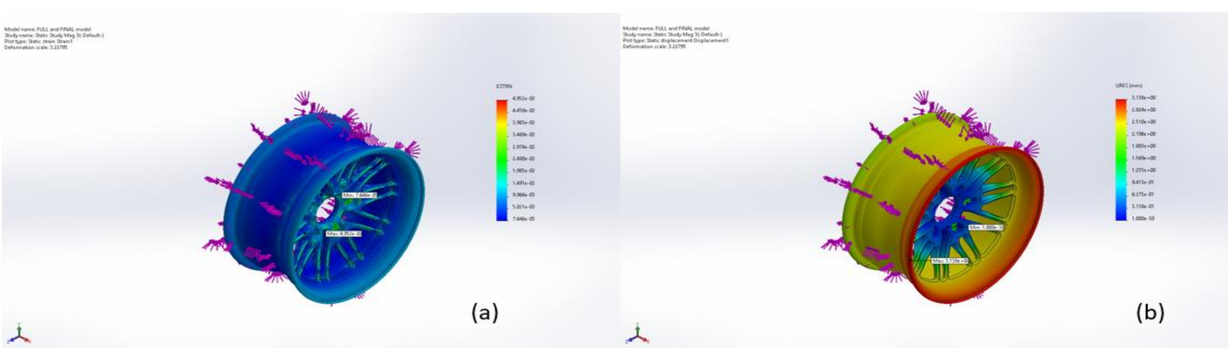

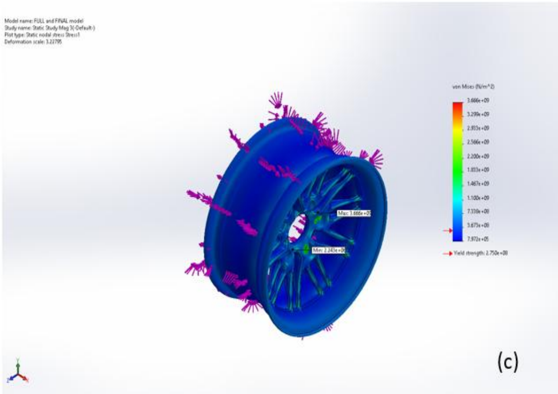

Figure 8. Stress-strain plots- Mg alloy wheel (a) Equivalent strain plot, (b) Displacement plot & (c) von-Mises stress plot

VI. CONCLUSIONS

The present work reveals the stress analysis for Al alloy and Mg alloy wheels under the uniformly distributed radial loading which is considered as an adverse condition. The von-Mises stresses induced in both alloy wheels are well within the true yield strength values of the materials. There is no deformation on the rim portion of the alloy wheels, thus indicating that the materials can sustain the maximum permissible air pressure combined with the radial load due to weight of car, passengers and luggage. The maximum von-Mises stresses are observed are at the curvature portion of ribs at the hub the alloy wheels. The highest stresses observed at these regions of the model may be indicative of stress singularities which are due to localized stress values diverging to infinity. The resultant displacement on the edges of the alloy wheels is observed to be abnormal. This may be due to the geometrical variations of the alloy wheels leading to stress concentration at the edge portion or deficient design. Thus, it indicates that the edge portion of the alloy wheels requires to be made stronger by way of providing more thickness. Mg alloy wheel has shown more resultant displacement on the edge which is due to low true yield strength compared to Al alloy wheel. The future work will focus on the coupled effect of static vehicle weight, cornering, braking, acceleration, and the tire inflation pressure on the alloy wheel to examine the strength of design.

REFERENCES

[1] Mandage, M. Sharma, A. Rayate, P. Kange, and N. Hirulkar, "Fatigue Life Estimation of an Aluminium Wheel Rim Using Finite Element Analysis," *International Journal of Scientific Advances Research and Technology*, vol. 2, pp. 30–33, 2016.

[2] K. S. Rao, M. Rajesh, and G. S. Babu, "Design and Analysis of Alloy Wheels," *International Research Journal of Engineering and Technology (IRJET)*, vol. 7, pp. 2036–2042, 2017.

[3] S. Das, "Design and Weight Optimization of Aluminum Alloy Wheel," *International Journal of Scientific Research Publications*, vol. 4, pp. 1–12, 2014.

[4] P. R. Raju, B. Satyanarayana, K. Ramji, and K. S. Babu, "Evaluation of Fatigue Life of Aluminium Alloy Wheels Under Bending Loads," *Fatigue & Fracture of Engineering Materials & Structures*, vol. 32, pp. 119–126, 2009.

[5] L. Wang, Y. Chen, C. Wang, and Q. Wang, "Fatigue Life Analysis of Aluminum Wheels by Simulation of Rotary Fatigue Test," *Strojniški Vestnik – Journal of Mechanical Engineering*, vol. 57, pp. 31–39, 2011.

[6] X. Wang and X. Zhang, "Simulation of Dynamic Cornering Fatigue Test of a Steel Passenger Car Wheel," *International Journal of Fatigue*, vol. 32, pp. 434–442, 2010.

[7] Z. Dong, X. Wang, X. Zhang, W. Lou, Y. Huang, and M. Zhong, "Fatigue Life Prediction for the Steel Passenger Car Wheel in the Dynamic Cornering Fatigue Test," *Strength of Materials*, vol. 52, pp. 662–682, 2020.

[8] F. Liu, *Mechanics and Mechanisms of Fracture: An Introduction*. Materials Park, OH, USA: ASM International, 2005, p. 15.

[9] *ASM Handbook, Volume 20: Materials Selection and Design*. Materials Park, OH, USA: ASM International, 1997, pp. 375–407.

[10] R. Powell, P. E. Krajewski, and A. A. Luo, "Magnesium Alloys for Lightweight Powertrains and Automotive Structures," in *Materials, Design and Manufacturing for Lightweight Vehicles*, P. K. Mallick, Ed. Cambridge, U.K.: Woodhead Publishing, 2010,

pp. 114–173, doi: 10.1533/9781845697822.1.114.

[11] R. Ohol, B. A. Parate, and D. Thakur, "Plastic Deformation of High Explosive Projectile 155 mm During Gun Launch Conditions Using Finite Element Method," *Defence Science Journal*, vol. 72, pp. 793–800, 2022, doi: 10.14429/dsj.72.18197.